Mem. S.A.It. Suppl. Vol. 1, 18

Memorie della
Supplementi

A parallel implementation of a new fast algorithm for N-body simulations

P. Londrillo[1], C. Nipoti[2],
and L. Ciotti[2]

[1] INAF – Osservatorio Astronomico di Bologna, via Ranzani 1, 40127 Bologna, Italy e-mail: londrillo@bo.astro.it

[2] Dipartimento di Astronomia, Università di Bologna, via Ranzani 1, 40127 Bologna, Italy e-mail: nipoti@bo.astro.it, ciotti@bo.astro.it

Abstract.
A new, momentum preserving fast Poisson solver for N-body systems sharing effective $O(N)$ computational complexity, has been recently developed by Dehnen (2000, 2002). We have implemented the proposed algorithms in a Fortran-90 code, and parallelized it by a domain decomposition using the MPI routines. The code has been applied to intensive numerical investigations of galaxy mergers, in particular focusing on the possible origin of some of the observed scaling relations of elliptical galaxies. We found that the Fundamental Plane is preserved by an equal mass merging hierarchy, while it is *not* in a scenario where galaxies grow by accretion of smaller stellar systems. In addition, both the Faber-Jackson and Kormendy relations are *not* reproduced by our simulations.

Key words. methods: N-body simulations – methods: numerical – galaxies: elliptical and lenticular, cD – galaxies: formation – galaxies: fundamental parameters

1. Introduction

In the last few years, fast algorithms for computing N-body interactions relying on the general multipole expansion techniques have been developed. These schemes, usually referred to as Fast Multipole Methods (FMMs, see, e.g., Greengard & Rokhlin 1987, 1997), are designed to have $O(N)$ computational complexity. However, it has been noted that only $O(N\log N)$ scaling is usually achieved in numerical implementation (see, e.g., Capuzzo-Dolcetta & Miocchi 1998, hereafter CM98). The $O(N\log N)$ operation count also characterizes the N-body codes based on tree algorithms, originally proposed by Barnes & Hut (1986, hereafter BH86). In addition, it has been shown by direct numerical tests that, for given accuracy, tree-codes are faster than the FMMs by a factor of ~ 4 (CM98). For this reason, most of the N-body codes currently used for astrophysical applications are based on

Send offprint requests to: P. Londrillo
Correspondence to: Osservatorio Astronomico di Bologna, via Ranzani 1, 40127 Bologna

the classical BH86 tree scheme, where the particle data are organized into a nested oct-tree cell structure. Interactions between distant particles are approximated by cell–particle interactions, and the distribution of the particles on each cell is represented by a multipole expansion, usually truncated to the quadrupole term.

Recently, a new scheme has been introduced (Dehnen 2000, 2002, hereafter D02), which can be seen as an original combination of the tree-based BH86 scheme and of the FMMs multipole expansion, truncated at a fixed low order level (the proposed $p = 3$ order results the optimal one). This scheme, implemented by the Author in a C++ code [named falcON, Force Algorithm with Complexity $O(N)$], results in a significant improvement over the existing BH86 tree-codes, in terms of uniform accuracy, linear momentum conservation, and CPU time performances. Moreover, the numerical tests presented in the D02 paper show that for an accuracy level $\epsilon \simeq 10^{-3}$, for the first time an *effective* $O(N)$ scaling in operation count, as predicted by the FMM theory, is in fact obtained. For these reasons two of us (P.L. and C.N.) have implemented this scheme in a new Fortran-90 code (FVFPS, a Fortran Version of a Fast Poisson Solver), and have then parallelized it by using the MPI procedures. A completion of the code to handle gas-dynamics using Euler equations and the AMR (Adaptive Mesh Refinement) techniques is under development. Here we briefly describe the main characteristics of Dehnen's algorithm, and we present our FVFPS implementation and its parallelization. The achieved accuracy level, the performances in terms of operation count speed-up, the effective $O(N)$ scaling, as well as the parallel scaling with the processors number, are then documented in numerical tests. Finally, we describe some interesting astrophysical applications of the code, in the context of the study of galaxy merging. Our version of the code is available upon request.

2. Dehnen's scheme

In the FMM approach, a system of particles is first organized in a oct-tree structure of nested cells, providing a hierarchical grouping of particles. For each pair of distant cells (A, B), the interactions between particles are then approximated by a Taylor expansion of the two-point Green function around the *geometrical center* of each cell by using spherical harmonics. In these cell-cell interactions the two-body symmetry of the exact Green function is preserved by the multipole approximation. In principle, a FMM-based scheme can achieve a prescribed accuracy ϵ by increasing the order p of the Taylor polynomial, and/or by lowering the expansion parameter $\eta \equiv r/R$ (where R is the distance between the two cell centers and r gives the typical size of a cell enclosing a particle group). Even if a formal, asymptotic scaling $O(N)$ is expected, the proposed algorithms in the original formulation (Greengard & Rokhlin, 1997) appear in fact to be less performing and of difficult application. Therefore, a first variant has been introduced in CM98, where the expansion order is kept fixed to $p = 2$, and only the η parameter controls the accuracy of the Taylor expansion. This approach takes advantage of the adaptivity of tree algorithms to select the pairs of cells (even belonging to different levels of refinements), which satisfy the opening criterium $r_{\rm crit}/R \leq \theta$, where θ is a preassigned control parameter. To improve the efficiency of the scheme, a new definition of the critical size $r_{\rm crit}(A, B)$, has been also introduced. However, even in this improved formulation, the FMM scheme results to be not competitive with the classical BH86 tree-code.

Dehnen's scheme basically develops along similar lines, but with some new ingredients, which in fact succeeded to improve the overall efficiency in a substantial way:

– the Taylor polynomial expansion is performed in Cartesian components, and the expansion centers are the center of

mass of each cell, as in the BH86 tree-code;
- a fixed expansion order $p = 3$ is chosen as optimal;
- a new definition of the critical radius $r_{\rm crit}$ is introduced for each cell, to optimize the adaptive selection of all pairs of well-separated cells;
- a new, mass dependent control parameter $\theta = \theta(M)$ has been introduced, that assures faster performances and a more uniform error distribution. The $\theta(M)$ function is given in implicit form by

$$\frac{\theta^5}{(1-\theta)^2} = \frac{\theta_{\rm min}^5}{(1-\theta_{\rm min})^2}\left(\frac{M}{M_{\rm tot}}\right)^{-\frac{1}{3}}, \quad (1)$$

where $\theta_{\rm min}$ (the minimum value of θ, associated with the total mass) enters as a new, preassigned control parameter, and where M is the total mass enclosed in a cell.

The resulting force solver is then organized as follows:

(a) As in the BH86 code, an oct-tree structure of nested cells containing particles is first constructed. A generic cell A, when acting as a gravity "source" is characterized by the position of its center of mass $\mathbf{X}_A$, by its critical size r_A, mass M_A, and by the quadrupole tensor Q_A. For the same cell A, when acting as a gravity "sink" a set of (twenty) Taylor coefficients C_A are used to store the potential and acceleration values at $\mathbf{X}_A$.

(b) To compute these coefficients, a new procedure for the tree exploration has been designed: starting from the root cell, all pairs of cells (A, B) satisfying the acceptance condition $(r_A+r_B)/R \leq \theta$, are looked for in a sequential way. When the condition is satisfied, each cell of the selected pair accumulates the resulting interaction contributions in $C_A(B)$ or $C_B(A)$. In case of nearby cells (not satisfying the acceptance condition), the bigger cell of the pair is splitted, and the new set of pairs are then considered. However, in order to avoid visiting the tree too deeply, some empirical conditions are adopted to truncate the sequence, by computing directly (exact) two-body forces for particles in the smallest cells. The Author, by using a stack structure to order the visited cell-pairs, has introduced a powerful and efficient new algorithm able to perform this *interaction phase* in the force computations.

(c) Finally, once all the cell-cell interactions has been computed and stored in the C_A array, a final step is needed to evaluate the gravitational potential and the accelerations of the particles in the (generic) cell A. This *evaluation phase* can be performed by a simple and fast $O(N)$ tree-traversal.

In our F-90 implementation of the scheme above, we followed rather closely the algorithms as described in D02: at this stage of development and testing, we have neither attempted to optimize our implementation, nor to look for particular tricks to save computational time.

To parallelize the force solver, we have adopted a straightforward strategy, by first decomposing the physical domain into a set of non-overlapping subdomains, each containing a similar number of particles (a few per cent of tolerance is allowed). The set of particles on each subdomain, S_k, is then assigned to a specific processing unit, P_k. Each processor builds its own tree [step (a)], and computes the interaction phase for all the particles in its subdomain [step (b)]. Steps (a) and (b) are executed in parallel. By ordering the processors in a one-dimensional periodic chain, it is then possible to exchange (particles and tree-nodes) data between them, by a "send_receive" MPI routine, in such a way that each processor can compute the interaction phase with the other subdomains. This phase is then performed by the following computational steps:

(i) The P_k processor sends its source-data to P_{k+s} and receives from the P_{k-s} a copy of its source-data, where $s = 1, 2, ...N_{\rm PE}/2$, and $N_{\rm PE}$ is the total number of processors.

(ii) At any given level s, each P_k computes, again in parallel, the interaction

phase with particles and cells of P_{k-s}. Mutuality of the interactions allows to evaluate, at the same time, the results of these interactions for cells and particles of processor P_{k-s} to be stored as sink-data.

(*iii*) These accumulated sink-data (acceleration for particles and Taylor's coefficients for cells) are sent back to the P_{k-s} processor, while the corresponding sink-data of the P_k processor are received from processor P_{k+s} and added to the current P_k values. In this way, it is evident that by repeating step (*ii*) $N_{\rm PE}/2$ times and step (*iii*) $N_{\rm PE}/2-1$ times, the interactions of P_k particles with all other particles in the domain are recovered.

(*iv*) The final evaluation phase [step (c)], being fully local, is performed in parallel.

Besides the force solver, the N-body code has been completed by a leap-frog time integrator scheme, with a (uniform) time step size Δt determined adaptively using a local stability condition $\Delta t < 1/\sqrt{4\pi G\rho_{\rm max}}$, where G is the gravitational constant, and $\rho_{\rm max}$ the maximum of particle density. For typical simulations involving galaxy mergers, this adaptive (in time) step size keeps comparable to the value $T_{\rm dyn}/100$, where $T_{\rm dyn}$ represents a macroscopic dynamical time scale, and assures energy conservation with relative errors smaller than 0.1%.

3. Performances of the FVFPS code

We ran some test simulations in order to estimate the performances of our FVFPS code, and to compare it both with falcON and with the BH86 tree-code. We focus first on the analysis of the time efficiency in force calculation, considering (one–processor) *scalar simulations* of the N-body system representing a galaxy group, where each galaxy is initialized by a Hernquist (1990, hereafter H90) galaxy model. Values of the total number of particles N up to 2×10^6 are considered. The opening parameter given in eq. (1) is used by adopting $\theta_{\rm min}=0.5$, while for the BH86 code we used $\theta=0.8$: this choice results in comparable accuracies in the force evaluation. We ran our simulations on a Pentium III/1.133 GHz PC. For falcON and for the BH86 code we refer to the data published by D02, who used a Pentium III/933 MHz PC.

In Fig. 1 (left panel) we plot the time efficiency of the codes as a function of the number of particles; it is apparent from the diagram that FVFPS (solid line), as well as falcON (dashed line), reaches an effective $O(N)$ scaling, for $N\gtrsim10^4$. Our F-90 implementation results to be slower than the C++ version by a factor of ~1.5: we think that this discrepancy may be due to differences in the details of the implementation, and also reflects a better intrinsic efficiency of the C++ with respect to the F-90 for this kind of algorithms (especially for routines where intensive memory accessing is required). In the same diagram the data relative to the BH86 tree-code are also plotted (dotted line), and the $O(N\log N)$ scaling is apparent. As already documented in D02, it is remarkable how, for fixed N and prescribed accuracy, the BH86 tree-code is significantly slower than the new scheme: for example for $N\simeq10^5$ the FVFPS code is faster by a factor of ~8. Therefore, even if the present F-90 implementation does no yet appear to be optimal, it gives further support to the efficiency of the D02 scheme, independently of the adopted programming language and of the implementation details.

The accuracy in force evaluation is documented on the right panel of Fig. 1, where we plot, as a function of N, the mean relative error on the acceleration modulus (filled circles)

$$\left\langle\frac{\Delta a}{a}\right\rangle\equiv\frac{1}{N}\sum_{i=1}^{N}\frac{|a^i_{\rm approx}-a^i_{\rm direct}|}{a^i_{\rm direct}},\quad(2)$$

and the corresponding 99th percentile $(\Delta a/a)_99\%$ (empty squares), for FVFPS (solid lines) and, for comparison, in falcON (dashed lines). As usual, the reference acceleration values $a^i_{\rm direct}$ are evalu-

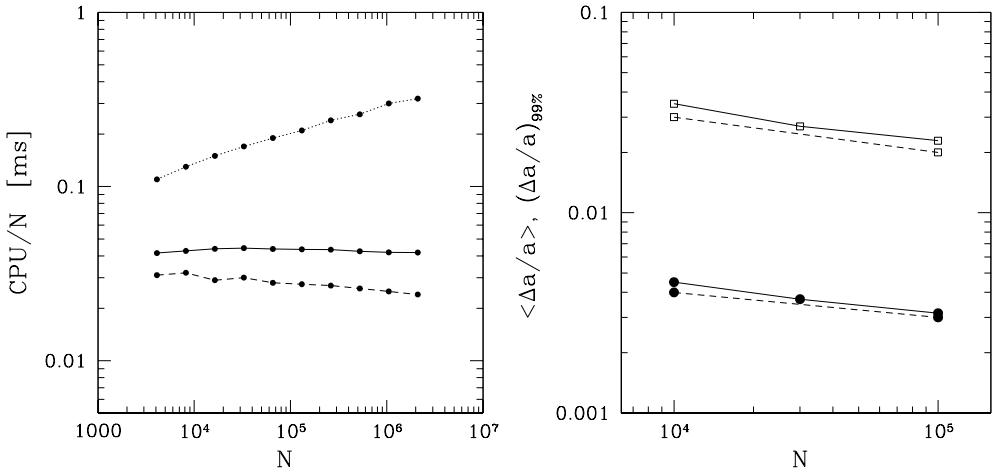

Fig. 1. *Left panel*: CPU time per particle as a function of total number of particles for BH86 tree-code (dotted line), falcON (dashed line; data from D02), and FVFPS (solid line). For the BH86 code $\theta = 0.8$, while in the last two cases $\theta = \theta(M)$, with $\theta_{\rm min} = 0.5$. *Right panel*: Mean error on the force calculation (filled circles) and the 99th percentile (empty squares), as a function of the number of particles in falcON (dashed line; data from D02), and in FVFPS (solid line).

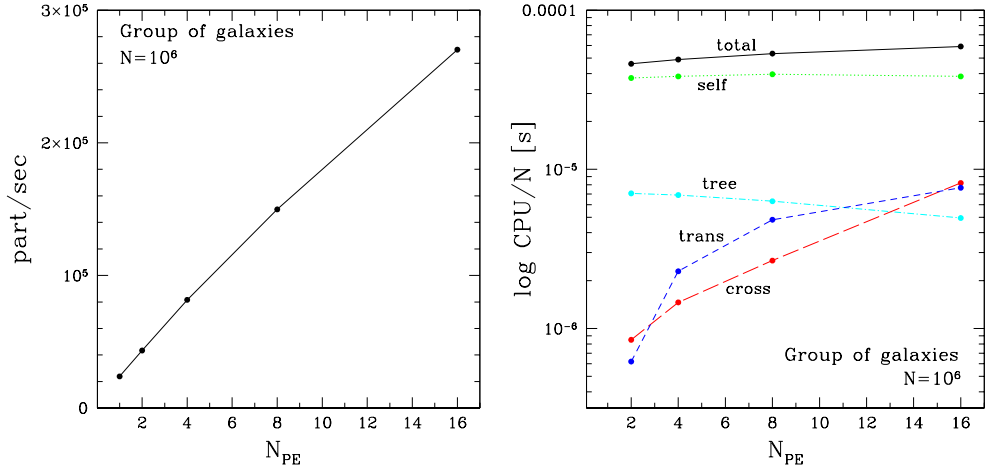

Fig. 2. *Left panel*: number of particle processed per second by the parallel version of the FVFPS code, as a function of the number of processors. The data refer to simulations of a group of galaxies with total number of particles $N = 1048576$. *Right panel*: CPU time per particle as a function of the number of processors for the same simulations in left panel. The different contributions are plotted (see text for an explanation).

ated by direct summation of the exact two-body Green function, while the approximated values are given with $\theta = \theta(M)$, and $\theta_{\rm min} = 0.5$. In this case, we have considered only simulations having a single H90 galaxy model. From the diagram it is apparent that, for both implementations, $\langle \Delta a/a \rangle$ and $(\Delta a/a)_9 9\%$ do not exceed a few 10^{-3} and a few per cent, respectively, assuring accuracies usually considered sufficient for astrophysical applications (see, e.g., CM98).

As outlined in the previous Section, we parallelized our code by using a domain decomposition with a load balancing essentially based only on particles number on each subdomain. This load balancing criterium seems in fact to work well, taking advantage of the intrinsic $O(N)$ scaling in the operation count of the basic scheme. In order to check the performance of the parallelized algorithm, we ran some simulations on the IBM Linux cluster (Pentium III/1.133 GHz PCs) at the CINECA center, in a range $N_{\rm PE} \leq 16$ in the number of processors. In this case the initial conditions are represented by a group of 8 one–component H90 galaxy models with a total number of particles $N = 1048576$. As can be observed in Fig. 2 (left panel), this parallelization is characterized by a rather well behaved linear scaling of the CPU time per particle versus $N_{\rm PE}$. This scaling can be better evaluated by considering the right panel of Fig. 2, where different contributions to the total CPU consumption are plotted. As expected, up to $N_{\rm PE} = 16$ the main contributions come by the tree building ("tree") and by the the force computation in each sub-domain ("self"), corresponding to the step (i) and (ii), respectively, of the parallel scheme outlined in the previous Section. The contributions coming from the force evaluation among particles belonging to different subdomains ("cross") and the cumulative time for all communication steps among processors ("trans"), which increase with $N_{\rm PE}$, keep smaller in the chosen range of parameters $(N, N_{\rm PE})$. Therefore, the $O(N)$ scaling of the base scheme, allows to estimate, for given N, the optimal configuration of the $N_{\rm PE}$ that can be used.

4. Simulations of galaxy merging

As an astrophysical application of the described FVFPS code, we consider here the study of the galaxy merging process. We checked the reliability of the numerical simulations performed with FVFPS for this kind of application (now time evolution is also considered), by running a few merging events, between spherically symmetric stellar systems, both with GADGET (Springel, Yoshida & White 2001), and with FVFPS. The results are in remarkable agreement: the remnants obtained with the two codes are practically indistinguishable for three-dimensional shape, circularized half–mass radius, circularized density and velocity dispersion profiles. As an illustrative example, in Fig. 3 we show the density profiles of the end–product of the merger obtained from the head–on parabolic encounter of two H90 models, with a total number of particles $N = 65536$ obtained with GADGET (empty symbols), and with FVFPS (filled symbols); note how also "minor" details, as the slope change in the density profile at $r \sim 10 r_{\rm M}$, are nicely reproduced. In addition, in both cases the change in total energy $\Delta E/E$ is smaller than 10^{-4} per dynamical time, over $100\, T_{\rm dyn}$. In this test, when using the FVFPS code, we adopted softening parameter $\varepsilon = 0.05$, initial time step $\Delta t = 0.01$, and (constant) $\theta = 0.65$; in the GADGET simulation we used $\varepsilon = 0.05$, $\alpha_{\rm tol} = 0.05$, $\Delta t_{\rm min} = 0$, $\Delta t_{\rm max} = 0.03$, $\alpha = 0.02$ (see Springel et al. 2001 for details), where the softening parameters and the time step parameters are in units of the galaxy core radius and dynamical time, respectively.

On the basis of the results of these tests, we used our N-body code to investigate with numerical simulations the effects of hierarchies of *dissipationless* galaxy mergers on the scaling relations of elliptical galaxies. This study is described in details in

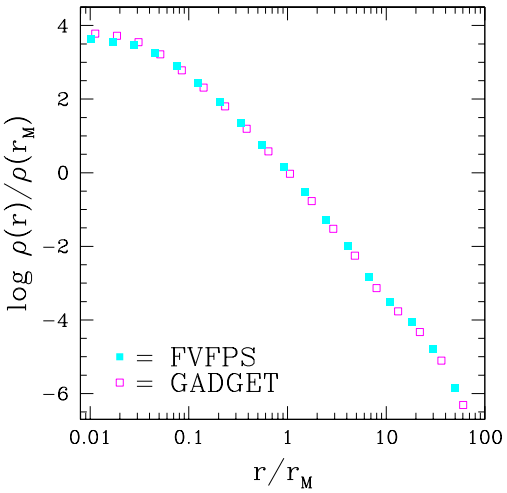

Fig. 3. Angle–average density profile of the remnant of the merging of two identical H90 galaxy models with FVFPS (full symbols), and with GADGET (empty symbols). $r_{\rm M}$ is the half–mass radius.

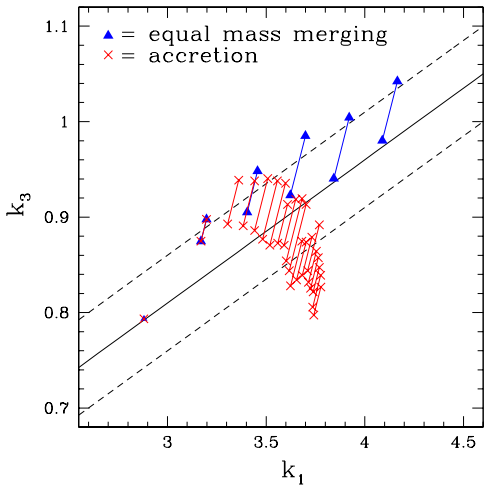

Fig. 4. The merging end–products in the (k_1, k_3) plane, where the solid line represents the edge–on FP relation with its observed 1-σ dispersion (dashed lines). Equal mass mergers are shown as triangles; crosses represent the accretion hierarchy. Bars show the amount of projection effects.

Nipoti, Londrillo & Ciotti (2002, hereafter NLC02). Here we report, as an example, the results relative to the effects of merging on the Fundamental Plane of elliptical galaxies (hereafter FP; Djorgovski & Davis 1987, Dressler et al. 1987). We considered a hierarchy of 5 equal mass mergers and a hierarchy of 19 accretion events, corresponding to an *effective* mass increase of a factor of $\sim$ 24 and $\sim$ 16, respectively: in the former case the successive generations are produced by merging pairs of identical systems obtained by duplicating the end–product of the previous step, while in the latter case each end–product merges with a seed galaxy. Each merging is produced in a head–on parabolic encounter. The seed galaxies are spherically symmetric one–component H90 galaxy models, with number of particles $N = 16384$ each. As a consequence of the merging hierarchy, the number of particles in the simulations increases with the galaxy mass: in the last merging of equal mass systems and of the accretion scenario, the total number of particles involved is of the order of 5.2×10^5 and 3.2×10^5, respectively.

In Fig. 4 we plot the results of equal mass merging and accretion simulations in the plane (k_1, k_3), where the *observed* FP is seen almost edge–on, with best–fit $k_3 = 0.15k_1 + 0.36$ (solid line) and scatter rms$(k_3) \simeq 0.05$ (dashed lines; see Bender, Burstein & Faber 1992). In the diagram the end–products of equal mass mergers and accretion are identified by triangles and crosses, respectively. The (common) progenitor of the merging hierarchies (point without bar) is placed on the edge–on FP. The straight lines in Fig. 4, associated with the merger remnants, represent the range spanned in the (k_1, k_3) space by each end–product, when observed over the solid angle, as a consequence of projection effects. It is interesting to note that for all the end–products the projection effects are of the same order as the observed FP dispersion. In addition it is also apparent from Fig. 4

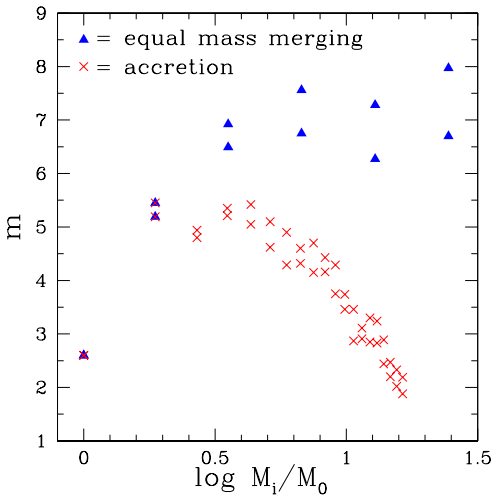

Fig. 5. Sersic best fit parameter m vs. total stellar mass of the end–products at stage i of the merging hierarchy. Symbols are the same as in Fig. 4

how, in case of equal mass merging, k_3 and k_1 increase with merging in a way full consistent with the observed FP tilt and thickness. On the other hand, in the case of accretions, after few steps the end–products are characterized by a k_3 *decreasing* for increasing k_1, at variance with the FP slope and the trend shown by the end–products of equal mass mergers. As a consequence, the last explored models (corresponding to an effective mass increase of a factor ~ 16) are found well outside the FP scatter.

The different behavior of the end–products in the two scenarios is due mainly to effects of *structural non–homology*. This is clearly shown by an analysis of the projected stellar mass density profiles of the end–products. In fact, we fitted (over the radial range $0.1 \lesssim R/\langle R\rangle_e \lesssim 4$) the projected density profiles of the end–products with the Sersic (1968) $R^{1/m}$ law, and in Fig. 5 we plot the best fit parameter m as a function of the total mass of the systems, for equal mass mergers (triangles) and accretion (crosses). Clearly, the best-fitting m depends on the relative orientation of the line–of–sight and of the end–products of the simulations: the two points for each value of the mass in Fig. 5 show the range of values spanned by m when projecting the final states along the shortest and longest axis of their inertia ellipsoids. In case of equal mass merging, the trend is m increasing with galaxy mass, as observed in real elliptical galaxies (see, e.g., Bertin, Ciotti & Del Principe 2002 and references therein). On the contrary, in case of accretion the best Sersic m parameter decreases at increasing mass of the end–product, a behavior opposite to what is empirically found.

As it is well known, elliptical galaxies follow, besides the FP, also other scaling relations, such as the Faber–Jackson (hereafter FJ, Faber & Jackson 1976), and the Kormendy (1977) relations. It is remarkable that, in our simulations, both the equal mass merging and the accretion hierarchies fail at reproducing these two relations. In fact, the end–products have central velocity dispersion lower, and effective radius larger than what predicted by the FJ and the Kormendy relations, respectively. In case of equal mass mergers, these two effects curiously compensate, thus preserving the edge–on FP. In other words, the remnants of *dissipationless* merging like those described, are *not* similar to real elliptical galaxies, though in some cases they reproduce the edge–on FP (see NLC02 for details).

5. Conclusions

The main results of our work can be summarized as follows:

- Our implementation of the D02 scheme in a F-90 N-body code (FVFPS) has effective $O(N)$ complexity for number of particles $N \gtrsim 10^4$, though its time efficiency is lower by a factor of ~ 1.5 than Dehnen's C++ implementation.
- As shown by numerical tests, the parallelized version of the FVFPS code has good scaling with the number of processors (for example for numbers of parti-

cles $N \simeq 10^6$, at least up to 16 processors).
- We found very good agreement between the results of merging simulations performed with our FVFPS code and with the GADGET code.
- From an astrophysical point of view, our high resolution simulations of hierarchies of *dissipationless* galaxy mergers indicate that *equal mass* merging is compatible with the existence of the FP relation. On the other hand, when an *accretion* scenario is considered, the merger remnants deviate significantly from the observed edge–on FP (see also NLC02).
- The different behavior with respect to the FP of the merger remnants in the two scenarios is a consequence of structural non–homology, as shown by the analysis of their projected stellar density profiles.
- In any case, the end–products of our simulations fail to reproduce both the FJ and Kormendy relations. In the case of equal mass merging, the combination of large effective radii and low central velocity dispersions maintains the remnants near the edge–on FP.

Acknowledgements. We would like to thank Walter Dehnen for helpful discussions and assistance. Computations have been performed at the CINECA center (Bologna) under the INAF financial support. L.C. was supported by MURST CoFin2000.

References

Barnes J. E., Hut P., 1986, Nature, 324, 446 (BH86)
Bender R., Burstein D., Faber S. M., 1992, ApJ, 399, 462
Bertin G., Ciotti L., Del Principe M., 2002, A&A, 386, 1491
Capuzzo-Dolcetta R., Miocchi P., 1998, Journal of Computational Physics, 143, 29 (CM98)
Dehnen W., 2000, ApJ, 536, L39
Dehnen W., 2002, Journal of Computational Physics, preprint (astro-ph/0202512), (D02)
Djorgovski S., Davis M., 1987, ApJ, 313, 59
Dressler A., Lynden-Bell D., Burstein D., Davies R.L., Faber S.M., Terlevich R., Wegner G., 1987, ApJ, 313, 42
Faber S.M., Jackson R.E., 1976, ApJ, 204, 668
Greengard L., Rokhlin V., 1987, Journal of Computational Physics, 73, 325
Greengard L., Rokhlin V., 1997, Acta Numerica, 6, 229
Hernquist L., 1990, ApJ, 356, 359 (H90)
Kormendy J., 1977, ApJ, 218, 333
Nipoti C., Londrillo P., Ciotti L., 2002, MNRAS, submitted (NLC02)
Sersic J.L., 1968, Atlas de galaxias australes. Observatorio Astronomico, Cordoba
Springel V., Yoshida N, White S.D.M., 2001, New Astronomy, 6, 79